Dealing with the cigar: preliminary performance estimation of an INGOT WFS

Valentina Viotto, Elisa Portaluri, Carmelo Arcidiacono, Roberto Ragazzoni, Maria Bergomi, et al.

Valentina Viotto, Elisa Portaluri, Carmelo Arcidiacono, Roberto Ragazzoni, Maria Bergomi, Simone Di Filippo, Marco Dima, Jacopo Farinato, Davide Greggio, Demetrio Magrin, Luca Marafatto, "Dealing with the cigar: preliminary performance estimation of an INGOT WFS," Proc. SPIE 10703, Adaptive Optics Systems VI, 107030V (10 July 2018); doi: 10.1117/12.2313219

Event: SPIE Astronomical Telescopes + Instrumentation, 2018, Austin, Texas, United States

Dealing with the cigar: preliminary performance estimation of an INGOT WFS

Valentina Viotto*[ab], Elisa Portaluri[ab], Carmelo Arcidiacono[bc], Roberto Ragazzoni[ab], Maria Bergomi[ab], Simone Di Filippo[bd], Marco Dima[ab], Jacopo Farinato[ab], Davide Greggio[ab], Demetrio Magrin[ab], Luca Marafatto[ab]

[a]INAF – Osservatorio Astronomico di Padova, Vicolo dell'Osservatorio 5, 35122, Padova, Italy

[b]ADONI – ADaptive Optics National laboratory in Italy

[c]INAF – Osservatorio Astrofisico e Scienza dello Spazio, Via Gobetti 93/3, 40129, Bologna, Italy

[d]Dipartimento di Matematica e Fisica, Università degli Studi Roma Tre, Roma, Italy

ABSTRACT

As LGSs come from an excited cigar-shaped region in the sodium layer, they do not behave as point-like sources, therefore a new class of WFSs has been proposed to account for such elongation: the Ingot WFSs, the LGS-counterpart of a pyramid WFS. As they appear to be very promising, here we summarize the main reasons and goal of such a LGS-dedicated WFS and present the concept behind the code developed to produce numerical simulations, exploring the space of parameters. We report different approaches for the approximation of the extended source and the model adopted for the ingot prism simulation.

Keywords: Laser guide star, wavefront sensing, adaptive optics

1. INTRODUCTION

The Laser Guide Stars (LGSs, [1]) are useful artificial sources, introduced to replace Natural Guide Stars (NGSs) in star poor regions, to produce artificial references for Adaptive Optics (AO) compensation. It is known, however, that they do not behave as point-like sources, because the emission comes from an excited cigar-shaped region in the sodium layer. While this consideration was already clear from geometrical approximation estimations, the actual impacts of the LGS extended shape, which changes according to the sub-aperture position inside the pupil, and of the variable thickness and homogeneity of the sodium layer, have been investigated through simulations and confirmed by on-sky observations, which experienced issues as spot truncation and sensitivity variation.

The Ingot wavefront sensor (I-WFS) has been recently proposed[2] to account for LGSs actual shape. As this technique appears to be very promising to solve the geometrical issues, an estimation of the expected performance shall be evaluated, compared with a "classical" Shack-Hartmann wavefront sensor (SH-WFS, [3]) approach. Here we present the preliminary analytical simulation code, which aims to give performance estimation, exploring the space of parameters, for trade-off purposes.

2. LGS SOURCE PECULIARITIES

When trying to conceive a new concept for a LGS-dedicated WFS, one should consider all the characteristics of the source itself, so to optimize the WFS design to the actual goal, e.g. a perfectly achromatic design would not give any benefit with respect to any other design, since the source is intrinsically monochromatic.

Both theory and on-sky demonstrations already pointed out several LGS characteristics, which are already taken into account in the relative AO modules designs. These are the finite distance of the source, the cone effect, the un-sensitivity to very low order modes[4]. For these reasons, we know that the WFS focal plane will be in a different position than the scientific one, that we need more LGSs to fill a meta-pupil, if compared to a very good NGSs asterism, and that we still need to provide an NGS channel to retrieve low-order modes aberrations.

*valentina.viotto@inaf.it

Adaptive Optics Systems VI, edited by Laird M. Close, Laura Schreiber,
Dirk Schmidt, Proc. of SPIE Vol. 10703, 107030V · © 2018 SPIE
CCC code: 0277-786X/18/$18 · doi: 10.1117/12.2313219

In a similar way, when conceiving a LGS-dedicated WFS, we should take into account also the other characteristics of the LGS, especially the fact that it is not a point-like source, for which the most used WFSs have been conceived and optimized.

2.1 Sodium layer thickness

The Sodium layer, located at about 90 km of altitude, allow us to produce the LGSs. This layer, however, is known to have a certain thickness and a certain density distribution, both varying with time. For this reason, the LGS is an extended elongated object, with a given orientation in the sky. In a focal plane WFS, like the SH-WFS, the spot will be only partially in focus, since the source extension along the optical axis (Z-axis in the following) is not negligible with respect to the LGS altitude. In particular, when trying to select the best focal plane orthogonal to the chief ray, only the central part of the source will be actually in-focus, while its extremities will be defocused (see Figure 1).

Several campaigns have been carried out to characterize the Sodium layer and its variability[5], so to understand which is their contribution to the error budget of e.g. a SH-WFS, and to clarify if this contribution would be acceptable or not for different classes of telescope. While a SH-WFS for LGS in wide pupil telescopes seems still to be feasible and reliable[6], with some caveat like the spot truncation (to avoid cross-talk between the signal in adjacent sub-apertures), a different approach could instead optimize the 1:1 matching between the source and the WFS used to sense it, in order to avoid the need of tricks to convert an extended object into a smaller one. The first goal for the ingot design, then, is to make the source image really focus on the element used to discriminate the parts of the wavefront affected by different local first-derivative, so to increase the signal-to-noise of the measurement.

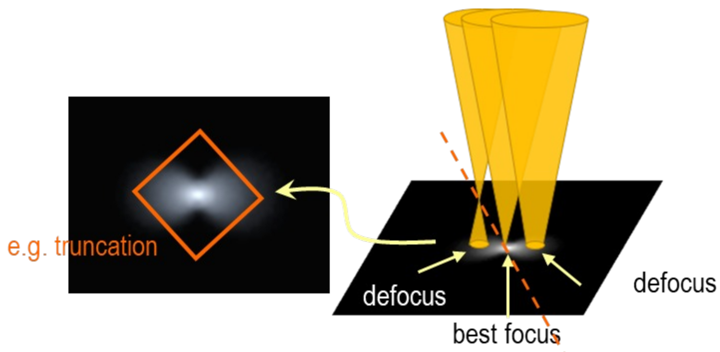

Figure 1. Effect of selecting the best focal plane orthogonal to the chief ray for a LGS re-imaging system.

2.2 Pupil Plane wavefront sensing for LGS

Another thing which could be considered in a LGS-dedicated WFS design is the advantage of selecting a pupil plane WFS approach. In addition to general pros like the ability to somehow sense differential piston in the entrance wavefront, the pupil plane WFS solution also allows the system to optimize the pixels occupation. To sample each sub-aperture, in fact, a SH-WFS (as an example of focal plane WFS) needs a number of pixels, which is large enough to Nyquist sample the smallest re-imaged spot (which has an angular size comparable to the one of the SH focal spots in the equivalent NGS wavefront sensing), but also the minimum field of view needed to include the most elongated spot, whose size will depend on the truncation applied in a previous focal plane. The typical number of needed pixels for each sub-aperture in a SH-WFS for a LGS at a ELT-like telescope is of the order of 10x10 pixels^2, while the P-WFS (mentioned as an example of pupil plane WFS), only needs 4 pixels.

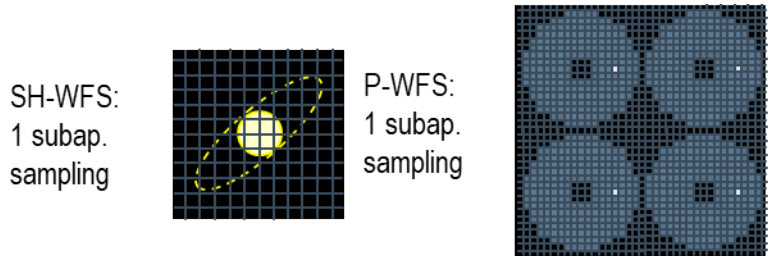

Figure 2. Difference in pixels occupation for a SH-WFS (*left*) and a P-WFS (*right*), in the LGS sensing case. In the SH-WFS focal plane, re-imaged spots have different angular sizes: the smallest (solid line) and the largest (dashed line) spots are reported.

2.3 LGS shape as seen from different sub-apertures

One of the characteristics, often referred to as a limitation, of the LGSs is the different solid angle under which each sub-aperture in the entrance pupil sees them. While sub-apertures close to the laser launcher identify the LGS as a source, which mainly extends along the Z-axis, sub-apertures located at the farthest limit of the pupil from the same launcher see the LGS as an object, which also extends in the plane parallel to the pupil itself (XY-plane, in the following). In a SH-WFS, this produces re-imaged spots with different sizes, depending on the positions of the sub-apertures that generate them. The spot elongation, for a four-quadrant-based WFS like the SH-WFS (but also the Pyramid WFS), translates into a decrease in the sensitivity of the signal to the local wavefront first order derivative, which will then be dependent on the relative sub-aperture position on the pupil and on the LGS orientation. This effect gets stronger while the telescope pupil diameter increases.

3. A SIX-FACES PRISM

To take into account the LGSs characteristics, reported before, the heart of the I-WFS is a weird-shaped prism, which faces the incoming light with six separated areas, differently deviating (by reflection and/or refraction) the incident beams so that a dedicated pupil re-imager can produce six pupils on the pupil plane. The 3-D shape of the Ingot allows to fit the LGS 3-D image both along the Z axis and in the XY plane, sampling it in three parts along the star elongation direction in the XY plane and in 2 parts (like a four-quadrant) in the other direction. Figure 3 reports the conceptual shape of the Ingot prism (a), and its projection, as seen from different sub-apertures on the entrance pupil (b, c). One can see that in case b), the sub-aperture close to the LGS launcher will only illuminates four out of the six faces of the prism, with a close-to-circular spot, like in a Pyramid WFS, while in case c), the sub-aperture that receives the LGS light from the largest solid angle will then produce an elongated spot covering the six faces.

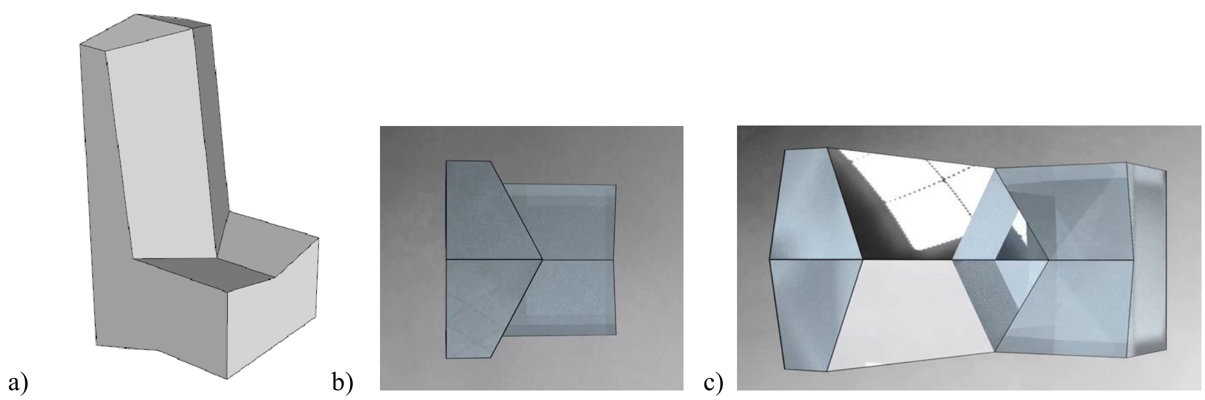

Figure 3. a) Ingot prism solid shape. b) Ingot prism as seen from sub-apertures close to the laser launcher position. c) Ingot prism as seen from sub-apertures far from the laser launcher position.

The six separated beams will then be re-imaged into six corresponding pupils, like in the P-WFS. The signals will be then obtained from the pupils in a 6-quad-like style. While the light on the pupils produced by the four lateral faces will contribute to give information on the wavefront derivative along both the axis, the light in the central two faces (present in case c) of Figure 3) only contributes to the derivative signal in the direction orthogonal to the spot elongation, under the assumption that the central faces mostly carry noise for this signal[7].

Since the design of the Ingot prism is optimized to match the LGS image geometrical characteristics, when the Sodium layer thickness changes, and the actual size of the source varies, the LGS image could not match anymore the ingot prism geometry. Figure 4 shows how this variation can affect the pupils illumination, in its extreme cases.

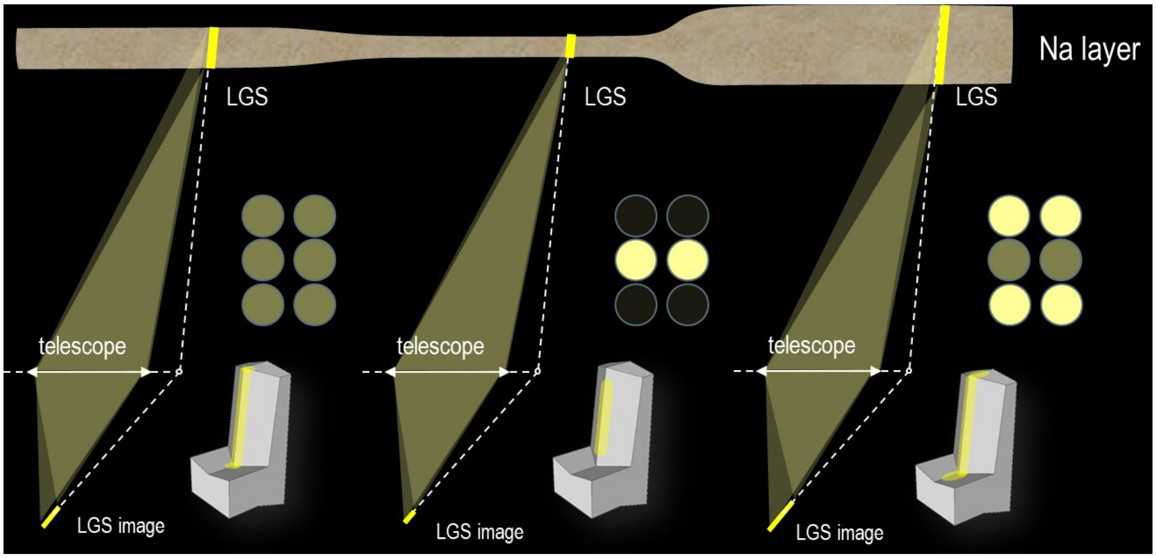

Figure 4. Effect of sodium layer variation on the LGS image matching the Ingot prism.

For this reason, we assume to have more ingot prisms for a single I-WFS, to be selected depending on the sodium layer thickness. The number of prisms needed shall be evaluated with a dedicated simulation to estimate the I-WFS performance sensitivity to the variation of the sodium layer profile FWHM.

4. INGOT WFS SIMULATION

The main purpose of the I-WFS simulation we carried out is to estimate, with an IDL code, the preliminary I-WFS performance using a geometric ray-tracing-like approach, in which the effect of diffraction is not included (except for the re-imaged size of the source, produced by the LGS sampling). This choice has been made, as this stage, to have a complete control on what is happening in the focal plane volume, which would be complicated to sample with Fourier Transforms, since the ingot prism extends far from the nominal focal plane (this would include fractional Fourier Transforms too).

In this simplified approach, the extended source is simulated as composed by a number of point-like sources, with a given spatial separation, so to sample the full cigar, both in the Z and in the XY directions (see Figure 5 as an example).

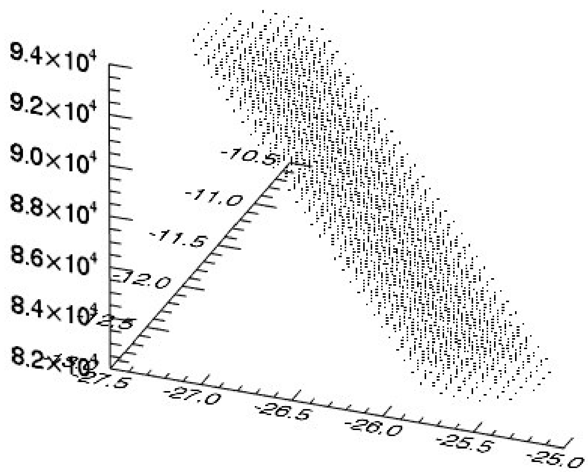

Figure 5. Example of LGS sampling in the sky. Units are meters.

Each point-like source produces *N* counts on the pupils, where *N* is the number of sub-apertures on the entrance pupil. The simulation considers as inputs the wavefront shape (which is actually retrieved from a turbulence profile, assuming frozen atmosphere and considering the cone effect), and the ELT pupil shape, sampled with a 0.1 m density. Position of the laser launcher, LGS orientation with respect to the entrance pupil and Ingot prism sizes and angles are input parameters too.

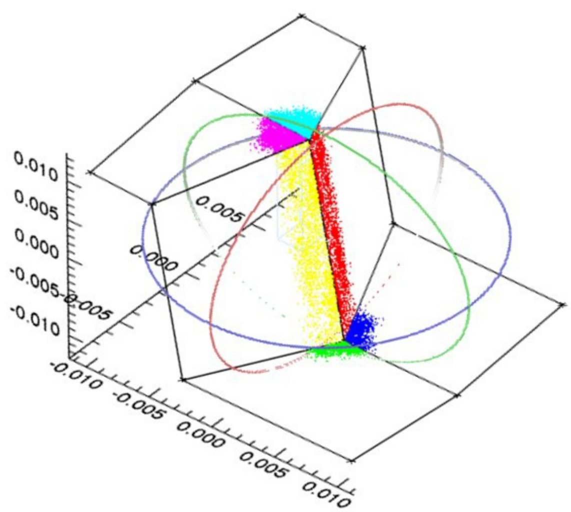

Figure 6. Ingot prism illuminated by incoming rays. A low cigar sampling and number of rays are reported for clarity sake. Units in the picture are meters, estimated for an ELT LGS projection, assuming a F/5 focal plane.

The prism is then built as composed by six quadrilaterals, defined in the 3D space, in the area of the telescope focal plane. Each pupil sub-aperture generates a ray for each point-like source illuminating it, perpendicular to the incoming wavefront, which intersects only one of the six faces of the prism. This allows to select which pupil the ray will illuminate. Figure 6 shows an example (with a limited number of rays and point-like sources, for sake of clarity) of a bundle of rays, sampling a LGS and illuminating the prism, given an incoming Von Karman-like aberration.

4.1 Current limitations in the simulation

The current main limitation in the simulation comes from the LGS sampling. The sampling already showed in Figure 4 is characterized by a regular grid, in the X-Y plane, replicated at different altitudes, following the LGS orientation. In the ray-tracing approach, however, the discretization of the source translates into a pattern in the signal, since no diffraction is there to smear out the pupils images. This give issues when inverting the interaction matrix to retrieve the reconstructor. This effect currently prevents us to produce high order modes reconstructors. In Figure 7, an example of the patterns one can see in the signals, if the source sampling is too poor, is reported for the Tilt signal case.

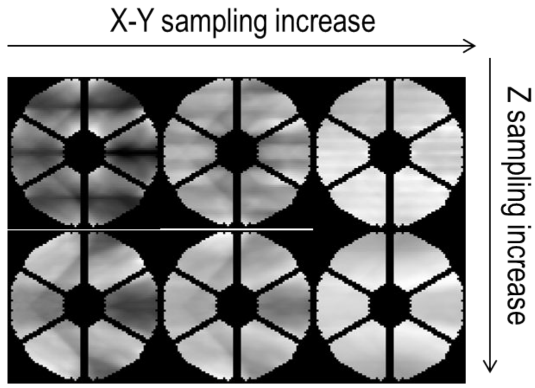

Figure 7. Example of Tilt signal variation as a function of the LGS source sampling in the X-Y plane and along altitude (Z).

These considerations would push to the use of a fine sampling of the LGS, with a very high number of point-like sources, which, unfortunately, make the simulation run very slowly. For this reason, in the future, we are going to evaluate the possibility to use different sampling approaches, like regular X-Y grids differently oriented for different altitudes, or completely different sources like disks, spheres or planes (see Figure 8).

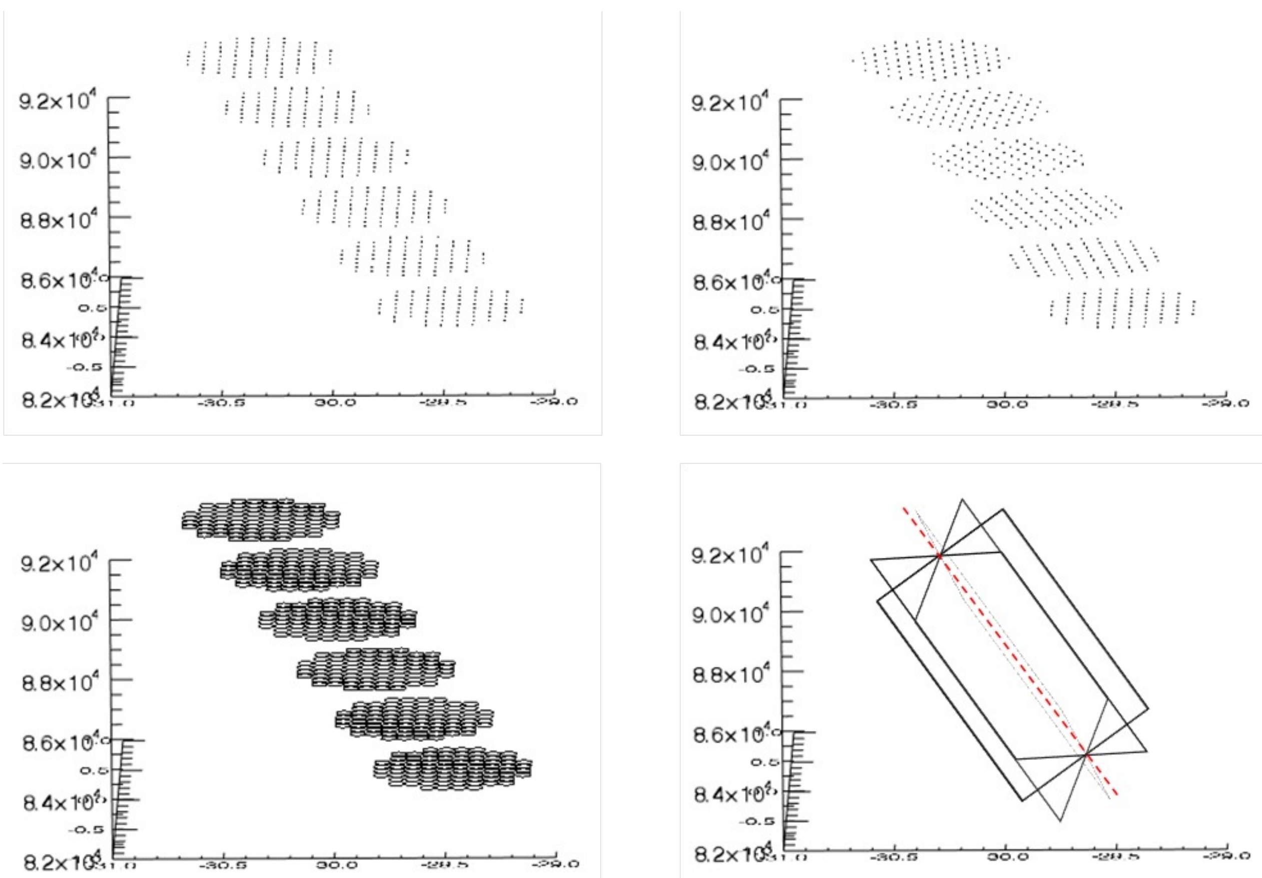

Figure 8. Different LGS sampling approaches to be evaluated.

For some of the sampling presented in Figure 8, it may be necessary to give up the ray-tracing approach.

Another important effect to consider is the uneven illumination of the re-imaged pupils, even if no incoming aberration is present. Figure 9 reports the simulated illumination (with FRED) of the pupils, when no aberration in the incoming wavefront is assumed.

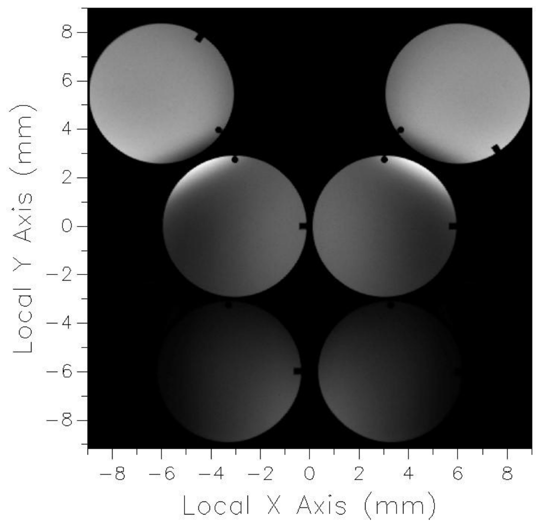

Figure 9. Illumination of I-WFS pupils, without incoming aberration.

This illumination pattern is due to three main effects:

- Intrinsic defocus of four over the six faces of the prism, with respect to the LGS image focal locus (Figure 10, *left*). This produces the horizontal gradient, which can be seen in the four pupils on the bottom of Figure 9. If a real defocus was present in the entrance wavefront, also the two pupils on the top should show the same horizontal gradient.
- Ingot prisms edges projections, as seen from different sub-apertures, are not parallel to X-Y axis (Figure 10, r*ight*). This translates into an excess/lack of light in corresponding parts of the pupils, reported in Figure 9.

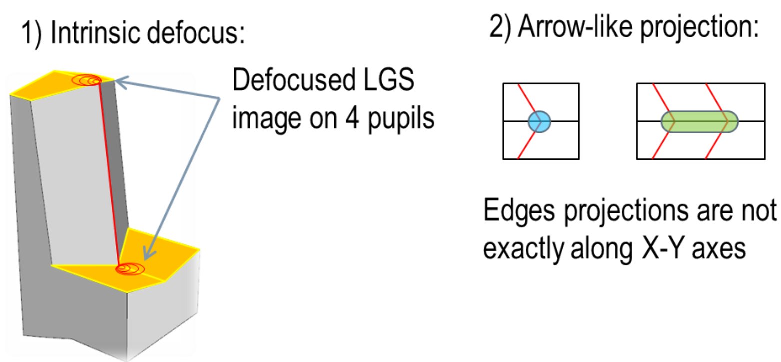

Figure 10. Sketches of the ingot prism geometrical characteristics affecting the pupil light distribution in absence of incoming aberration. *Left*: the defocus of LGS on external faces of the prism. *Right*: prism edges projection effect.

- A third effect is given by the fact that, while the light collected by sub-apertures far from the launcher illuminates all the six pupils, the one selected by the closest sub-aperture to the LGS launcher basically illuminates only four over the six pupils. For this reason a further gradient on the pupils, in the direction of the elongation of the LGS, is present.

5. NEXT STEPS

Next steps in the simulator development will be focused on the trade-off between LGS sampling, computational time needed, and the pupils signal uniformity. Some of the proposed sampling concepts, in particular, cannot be easily simulated with the currently selected ray-tracing approach, meaning that alternative ways to simulate the light passing through the ingot prism have to be evaluated.

Once a complete and reliable simulator will be in place, several analysis are foreseen. The first will be the study of the ingot performance sensitivity to the variations of the sodium layer profile, especially to evaluate the number of differently shaped ingot prisms needed in the WFS. This analysis is crucial also to estimate the effect of profile variability onto the light distribution inside the pupils, when no aberration is present in the incoming wavefront.

REFERENCES

[1] Foy, R. and Laberyrie, A., Booth, N. and Smith, A. S., "Feasibility of adaptive telescope with laser probe," A&A, 152, L29-L31 (1985).
[2] Ragazzoni, R., Portaluri, E., Viotto, V., Dima, M., Bergomi, M., Biondi, F., Farinato, J., Carolo, E., Chinellato, S., Greggio, D., Guilleuszik, M., Magrin, D., Marafatto, L. and Vassallo, D., "Ingot laser guide star wavefront sensing," AO4ELT5 Proceedings, (2017)
[3] Hardy, J., " Adaptive Optics for Astronomical Telescopes," New York: Oxford University Press, (1998)
[4] F. Rigaut and E. Gendron, "Laser guide star in adaptive optics - The tilt determination problem," A&A, 261, 677 (1992).
[5] Schreiber, L.; Diolaiti, E.; Arcidiacono, C.; Pfrommer, T.; Holzlöhner, R.; Lombini, M.; Hickson, P., "Impact of sodium layer variations on the performance of the E-ELT MCAO module," in Proc. SPIE, 9148, 91486Q (2014).
[6] Schreiber, l., et al, "The MAORY laser guide stars wavefront sensor: design status," this conference, (2018).
[7] Ragazzoni, R., Greggio, D., Viotto, V., Di Filippo, S., Dima, M., Farinato, J., Bergomi, M., Portaluri, E., Magrin, D., Marafatto, L., Biondi, F., Carolo, E., Chinellato, S., Umbriaco, G., and Vassallo, D., "Extending the pyramid WFS to LGSs: the INGOT WFS," this conference, (2018).